Indoor Target Tracking using Time Difference of Arrival Measurements in 3D

Yifan Xie, Seung Hyo Park and Taek Lyul Song
Department of Electronic Systems Engineering, Hanyang University, Ansan, Republic of Korea

Keywords: TDOA, 3D, Corrleated Measurement Noise, Cholesky, Target Tracking.

Abstract: Target tracking with time difference of arrival measurements usually encounters the problem of correlated measurement noises. When the sensor network utilizes the common reference sensor, the covariance matrix of the correlated measurement noises becomes off-diagonal such that the computational complexity of the inverse of the covariance matrix as well as the subsequent matrix operations increases proportionally to the cube of the sensor number. This makes target tracking algorithms inconvenient for practical applications, and an appropriate measurement noise decorrelation method is required. In multi-sensor environments, the parallel update and the serial update are applied for exploiting the measurements from different sensors. Although the two methods deliver the equivalent tracking performances in linear systems, this equivalence does not hold in nonlinear systems as linearizing the nonlinear functions leads to approximation error. Additionally, the requirements of the two methods for storage structure and computational resource allocations are different. This paper presents a target tracking algorithm which integrates the Cholesky decomposition to decorrelate the measurement noises for the serial update which shows computational efficiency. The tracking performance is evaluated by estimation accuracy, execution time.

1 INTRODUCTION

With the development of Ultra-wideband (UWB), indoor target tracking has emerged as a critical role in civilian and military applications (Taylor, 1994)(Eryildirim and Guldogan, 2016)(Alarifi et al., 2016). A UWB tracking system consists of multiple spatially distributed sensors and each sensor exploits the radio signals transmitted from the target to the sensors independently. The UWB tracking systems can be classified into different categories based on the measurement types: (1) received signal strength (RSS); (2) time of arrival (TOA); (3) time difference of arrival (TDOA), etc. The application of RSS based system is greatly constrained by the sensitivities in channel inconsistency (McCracken et al., 2013). The TOA based systems though deliver precise target position estimations, the device mounted on the target as well as all sensors must be precisely synchronized that difficult and expensive installations can be expected (Tuchler et al., 2005). Contrastively the TDOA based systems perform good accuracy and only require the reference sensor to be synchronized. These factors significantly simplifies the installation requirements and result in its popularity(Alarifi et al., 2016).

TDOA information is obtained from a wireless sensor network (WSN) composed of sensors that collect TOA of target signal. When one sensor is designated as the common reference sensor in the WSN, the time difference of arrival measurement can be obtained by making a difference between two TOA measurements. Most of the multi-sensor target tracking algorithm (Hashemipour et al., 1988)(You et al., 1999)(Gan and Harris, 2001) assume that the measurement noises from different sensors are uncorrelated as each sensor operates independently. But due to the common measurement noise of the reference sensor in the TDOA measurement generation procedure, the TDOA measurement noises are correlated. The correlated TDOA noise have been discussed in recent literatures (Ho and Chan, 1993)(Kaune et al., 2011)(Kim et al., 2012). However (Kaune et al., 2011) mainly addresses the target geolocation problem, the other problems such as the noise decorrelation and the target tracking are not investigated. In (Kim et al., 2012), the Gram-Charlier orthogonalization procedure is applied for noise decorrelation. Additionally, (Kim et al., 2012) models the TDOA measurement uncertainty more precisely by approximating the measurement likelihood to a Gaussian mixture such that better estimation results are achieved

Xie, Y., Park, S. and Song, T.
Indoor Target Tracking using Time Difference of Arrival Measurements in 3D.
DOI: 10.5220/0006882903800387
In *Proceedings of the 15th International Conference on Informatics in Control, Automation and Robotics (ICINCO 2018) - Volume 1*, pages 380-387
ISBN: 978-989-758-321-6

at the cost of computational resource and memory storage.

The algorithms of incorporating measurements from several sensors for target tracking usually apply two methods: parallel update and serial update (Bar-Shalom et al., 2011). These two methods are mathematically equivalent and have the same tracking performances in linear systems when the clutter measurements are not involved (Pao and Frei, 1995)(Pao and Trailovic, 2000). This equivalence does not hold in nonlinear systems as linearizing the nonlinear functions leads to approximation error. The parallel update stacks all measurements from different sensors into an augmented measurement vector. The state is updated simultaneously with the stacked vector that all measurements are utilized at once. The serial update utilizes the measurement from one sensor at a time. For nonlinear measurements, the order of updating is suggested to start from the measurement collected by the most accurate sensor to reduce the subsequent linearization errors(Duan et al., 2005)(Xie et al., 2016).

In this paper, the Cholesky decomposition (Bar-Shalom et al., 2004)(Duan et al., 2004)(Duan et al., 2005) is applied to transform the correlated TDOA noise into an equivalent one with uncorrelated TDOA noise. The decomposition matrix is utilized to create pseudo measurements and pseudo Jacobian matrix such that the target tracking can be implemented under uncorrelated noise situation. For computational efficiency, the serial update operates with pseudo measurements and pseudo Jacobian matrix is proposed in this paper.

The rest of the paper is organized as follows. Statements for the state vector formulation and the TDOA measurement generation are described in Section 2. Section 3 gives brief descriptions for the Cholesky decomposition method which is utilized for noise decorrelation. The target tracking methods using decorrelated TDOA measurements for the parallel update and the serial update are discussed in Section 4. Simulation study is given in Section 5, followed by the concluding remarks in Section 6.

2 PROBLEM STATEMENTS

In this section, state vectors for the target and sensors, as well as the correlations between TDOA measurements are presented.

2.1 State Vector

The target dynamics are modeled linear Gaussian in Cartesian coordinates. Under the additive noise assumption, the target kinematic at scan k is defined by

$$x_k = F_k x_{k-1} + \omega_k, \tag{1}$$

where $x_k = [x_k\ y_k\ z_k\ \dot{x}_k\ \dot{y}_k\ \dot{z}_k]^T$ is the target state vector with a position component $[x_k\ y_k\ z_k]^T$ and a velocity component $[\dot{x}_k\ \dot{y}_k\ \dot{z}_k]^T$, F_k is the transition matrix, and ω_k is the white Gaussian process noise with zero mean and covariance matrix Q_k.

In a sensor network with M sensors, the sensors are stationary with known positions and passively receive the signal emitted from the target. The state vector of the i-th sensor is $x_k^i = [x_k^i\ y_k^i\ z_k^i\ 0\ 0\ 0]^T$. A TDOA scenario is exemplified in Fig. 1, where

$$G = \begin{bmatrix} I_3 & 0_3 \end{bmatrix} \tag{2}$$

is the position projection matrix, I_n and 0_n denote the $n \times n$ identity and zero matrices respectively. The distance vector between the target and the i-th sensor is $r_{k,i} = Gx_k - Gx_k^i$, and $||r_{k,i}||$ is the corresponding Euclidean distance.

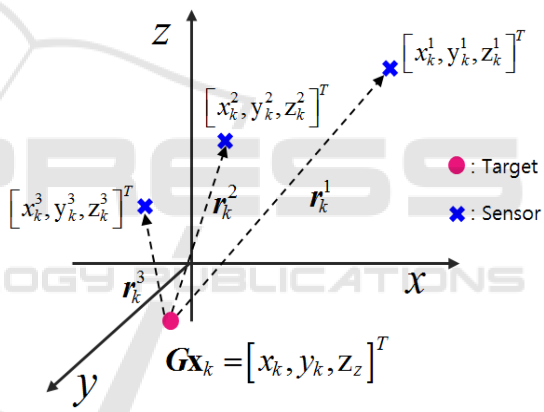

Figure 1: A TDOA scenario with 3 sensors.

2.2 TDOA Measurement

Denote sensor s_i $(i = 1, \dots, M)$ noise as $u_{k,i}$ with standard deviation σ_i and sensor s_1 is utilized as reference sensor. The TDOA measurement in time domain can be translated into a range difference by multiplying with the speed of light and is given by

$$\begin{aligned} z_{k,i} &= (||r_{k,i}|| - ||r_{k,1}||) + (u_{k,i} - u_{k,1}) && (3) \\ &= h_i(x_k) + \nu_{k,i}, \quad i = 2, 3, \dots, M && (4) \end{aligned}$$

where

$$h_i(x_k) = ||r_{k,i}|| - ||r_{k,1}||, \tag{5}$$

$$\nu_{k,i} = u_{k,i} - u_{k,1}, \tag{6}$$

$\nu_{k,i}$ is the TDOA measurement noise, $\nu_{k,i} \sim \mathcal{N}(0, \sigma_{1,i}^2)$ and $\sigma_{1,i}^2 = \sigma_1^2 + \sigma_i^2$.

At each scan k, $M-1$ TDOA measurements are generated from M passive sensors, which can be given in a stack form of

$$z_k = [z_{k,2}\ z_{k,3} \cdots z_{k,M}]^T. \tag{7}$$

The measurement equation for z_k is given by

$$z_k = h(x_k) + \nu_k, \tag{8}$$

$$h(x_k) = [h_2(x_k)\ h_3(x_k)\ \cdots\ h_M(x_k)]^T, \tag{9}$$

$$\nu_k = [\nu_{k,2}\ \nu_{k,3}\ \cdots\ \nu_{k,M}]^T, \tag{10}$$

where $\nu_k \sim \mathcal{N}(0, R_k)$ and R_k is the covariance matrix.

Due to the fact that all TDOA measurements are created under a common reference sensor, the TDOA measurements are correlated and the relevant covariance matrix becomes off-diagonal (Kaune et al., 2011). The covariance matrix R_k is given by

$$R_k = E[\nu_k \nu_k^T] = \begin{bmatrix} \sigma_{1,2}^2 & \sigma_1^2 & \cdots & \sigma_1^2 \\ \sigma_1^2 & \sigma_{1,3}^2 & \cdots & \sigma_1^2 \\ \vdots & \vdots & \ddots & \vdots \\ \sigma_1^2 & \sigma_1^2 & \cdots & \sigma_{1,M}^2 \end{bmatrix}. \tag{11}$$

Assume that all sensors are homogeneous with the same standard deviation of sensor noise σ_u, then eq (11) becomes

$$R_k = 2\sigma_u^2 \begin{bmatrix} 1 & 0.5 & \cdots & 0.5 \\ 0.5 & 0.5 & \cdots & 0.5 \\ \vdots & \vdots & \ddots & \vdots \\ 0.5 & 0.5 & \cdots & 1 \end{bmatrix} \triangleq 2\sigma_u^2 \Omega_k, \tag{12}$$

where matrix Ω_k is utilized for the TDOA measurement decorrelation in Section 3.

3 TDOA NOISE DECORRELATION

The covariance matrix R_k is off-diagonal and one can apply a linear transformation to diagonalize it. Since R_k is a real-valued symmetric positive-definite matrix, this transformation can be implemented by Cholesky decomposition (Bar-Shalom et al., 2004) and yields

$$R_k = L_k \Lambda_k L_k^T, \tag{13}$$

where L_k is a unit lower triangular matrix, $\Lambda_k = 2\sigma_u^2 I_{M-1}$ and I_n denotes an $n \times n$ identity matrix. Denote the (m,n)th elements in Ω_k and L_k as $\Omega_k^{(m,n)}$ and $L_k^{(m,n)}$, respectively. The decomposition matrix L_k is calculated by

$$L_k^{(m,n)} = \begin{cases} \sqrt{\Omega_k^{(m,n)} - \sum_{j=1}^{n-1} (L_k^{(n,j)})^2}, & m = n; \\ \left(\Omega_k^{(m,n)} - \sum_{j=1}^{n-1} L_k^{(m,j)} L_k^{(n,j)}\right) / L_k^{(n,n)}, & m > n; \\ 0, & otherwise. \end{cases}$$

As a consequence, the correlated TDOA measurement noise is transformed into an equivalent pseudo form with uncorrelated noise.

According to eqs (12) and (13), the covariance matrix R_k can be transformed into a form of

$$R_k = L_k E[I_u I_u^T] L_k^T, \tag{14}$$

together with eq (11) we can get

$$\nu_k = L_k I_u. \tag{15}$$

The stacked TDOA measurement z_k in eq (8) can be rewritten as

$$z_k = h(x_k) + L_k I_u. \tag{16}$$

Multiplying both sides of eq (16) with L_k^{-1}, the pseudo measurement z_k^p can be obtained by

$$z_k^p = L_k^{-1} z_k \tag{17}$$

$$= L_k^{-1} h(x_k) + I_u. \tag{18}$$

Then I_u becomes the pseudo measurement noise and follows

$$I_u \sim \sqrt{2} \begin{bmatrix} \mathcal{N}(0, \sigma_u) \\ \mathcal{N}(0, \sigma_u) \\ \vdots \\ \mathcal{N}(0, \sigma_u) \end{bmatrix}. \tag{19}$$

The covariance matrix of I_u is equivalent to Λ_k, which is diagonal and the pseudo measurement z_k^p is uncorrelated.

The Jacobian matrix of function $h(x_k)$ is given by

$$H_k = \frac{\partial h(x_k)}{\partial x_k}. \tag{20}$$

Similarly, multiplying both sides of eq (20) with L_k^{-1}, the pseudo Jacobian matrix is defined by

$$H_k^p = L_k^{-1} H_k. \tag{21}$$

4 TRACKING WITH DECORRELATED TDOA MEASUREMENTS

In this paper, an extend Kalman filter (EKF) is applied for target tracking with decorrelated TDOA measurements. Before the start of the EKF tracking recursion, the target should be localized based on the TDOA measurements received at the first scan for track initialization. After track initialization, the standard EKF prediction formulae are applied for track propagation. In the EKF update, the standard measurement and the Jacobian matrix are replaced by the pseudo ones for track status update. A flowchart of tracking procedure is illustrated in Fig. 2.

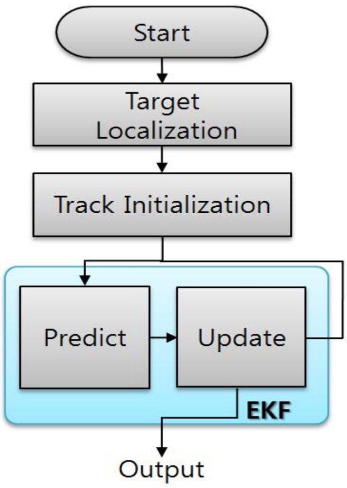

Figure 2: Flowchart of target tracking.

4.1 Track Initialization

The method in (Gillette and Silverman, 2008) of 3D geo-location using TDOA only measurements, which claims the initial target position can be localized effectively when at least 5 sensors are provided, is applied in this paper. The localized target positions $[\hat{x}_0\ \hat{y}_0\ \hat{z}_0]^T$ in three-dimension are further utilized for one-point track initialization (Challa et al., 2011). The initial track is parameterized by a initial mean of the target state x_0 and initial covariance matrix P_0 which are denoted as

$$x_0 = [\hat{x}_0\ \hat{y}_0\ \hat{z}_0\ 0\ 0\ 0]^T\,, \tag{22}$$

$$P_0 = \begin{bmatrix} 2\sigma_u^2 I_3 & 0_3 \\ 0_3 & v_{max}^2 I_3/3 \end{bmatrix}, \tag{23}$$

where v_{max} is the maximum target velocity determined by the designers. The initialized track is used as an input for the EKF recursion.

4.2 Parallel Update

In the parallel update, the track state is updated simultaneously with the stacked measurement z_k. The updated state is defined by its mean $\hat{x}_k$ and covariance $\hat{P}_k$. The input is a predicted state defined by its mean $\bar{x}_k$ and covariance $\bar{P}_k$:

$$\hat{x}_k = \bar{x}_k + K_k\left(z_k - h(\bar{x}_k)\right), \tag{24}$$

$$\hat{P}_k = \bar{P}_k - K_k H_k \bar{P}_k, \tag{25}$$

with

$$S_k = H_k \bar{P}_k H_k^T + R_k, \tag{26}$$

$$K_k = \bar{P}_k H_k^T S_k^{-1}, \tag{27}$$

where S_k is the predicted measurement error covariance with $(M-1)\times(M-1)$ dimension, K_k is the filter gain with $6\times(M-1)$ dimension.

4.3 Serial Update

Apparently the matrix size in the parallel update increases with the sensor number, which not only complicates the matrix operations but also requires more memory storages. But in practical applications, the computational resources in the UWB target tracking systems may not be able to support large-scale matrix operations especially for inverse and multiplication. In addition, the oversize matrices such as S_k and K_k also bring heavy storage burden such that practical implementations can be hardly realized. Contrastively the serial update does not operate on the entire stacked pseudo measurement z_k^p simultaneously, but update with every element in z_k^p iteratively. As a consequence, the reductions in both computational resource and memory storage can be expected.

In the m-th iteration of serial update, the pseudo Jacobian matrix, the pseudo measurement and the predicted measurement are denoted as $H_{k,m}^p$, $z_{k,m}^p$ and $\bar{z}_{k,m}$, respectively. The (m,n)th element in L_k^{-1} is denoted as $L_k^{-1}(m,n)$. The updated track state is defined by mean $\hat{x}_{k,m}$ and covariance $\hat{P}_{k,m}$, which are further regarded as the predict mean and covariance for the next iteration. The iteration proceeds until the exhaustiveness of pseudo measurements. The pseudo-code for serial EKF update is shown in Algorithm 1, where matrices $S_{k,m}$ and $K_{k,m}$ reduce to sizes of 1×1 and 6×1 compared to S_k and K_k.

Algorithm 1: Serial EKF update.

for $m = 1 : M-1$ **do**
  $H_{k,m}^p = [0\,0\,0\,0\,0\,0]\,,\ \bar{z}_{k,m} = 0,\ z_{k,m}^p = 0$
  for $n = 1 : m$ **do**
    $H_{k,n} = \frac{\partial h_n(x_k)}{\partial x_k}|_{x_k = \bar{x}_k}$
    $H_{k,m}^p = H_{k,m}^p + L_k^{-1}(m,n) H_{k,n}$
    $\bar{z}_{k,m} = \bar{z}_{k,m} + L_k^{-1}(m,n) h_n(\bar{x}_k)$
    $z_{k,m}^p = z_{k,m}^p + L_k^{-1}(m,n) z_{k,n}$
  end for
  $S_{k,m} = H_{k,m}^p \bar{P}_k (H_{k,m}^p)^T + 2\sigma_u^2$
  $K_{k,m} = \bar{P}_k (H_{k,m}^p)^T S_{k,m}^{-1}$
  $\hat{x}_{k,m} = \bar{x}_k + K_{k,m}\left(z_{k,m}^p - \bar{z}_{k,m}\right)$
  $\hat{P}_{k,m} = \bar{P}_k - K_{k,m} H_{k,m}^p \bar{P}_k$
  $\bar{x}_k = \hat{x}_{k,m}$
  $\bar{P}_k = \hat{P}_{k,m}$
end for

4.4 Implementation Issues

The application of the Cholesky decomposition does not bring complicate matrix operations such as the matrix inverse of L_k. It is shown that the inverse of Cholesky decomposition matrix L_k of the correlated measurement noise can be predetermined and the elements $L_k^{-1}(m,n)$ of L_k^{-1} are invariant as the total sensor number M in one network is fixed. Therefore the elements $L_k^{-1}(m,n)$ can be pre-calculated off-line and stored in the memory. When $L_k^{-1}(m,n)$ is involved in the calculations of $H_{k,m}^p$, $z_{k,m}^p$ and $\bar{z}_{k,m}$, the relevant data can be read from the memory and utilized immediately such that computational load is relieved. Contrastively the parallel update utilizes an augmented measurement vector which stacks all the available TDOA measurements for track update. This not only brings more burden for storage management but also makes it computationally inefficient since the matrix operations for high dimensions are much more intractable.

Additionally, the serial update exhibits advantages in practical implementations. Since the sensor measuring performance can be affected by signal interference or glint noise, a part of all sensor measurements are selected for tracking performance optimality. As a consequence, the number of validated sensors becomes time variant. The matrix size in parallel update has to be modified accordingly in time. However, the only modification in serial update is the iteration number, which shows more conveniences for practical installations.

As the computational efficiency is important in practical applications, the computational load dominates the criterion of update scheme selection while the tracking performances are similar. The serial update utilizes the measurement from one sensor at a time that the computations in one iteration can be significantly reduced since the high dimensional matrix operations are avoided. The serial update also enables to distribute the computations uniformly according to the TDOA measurement number as shown in Fig. 3. The iteration number can be flexibly adjusted that a trade-off between the tracking performance and computational requirements as long as the target observability is satisfied, i.e., the iteration number should be at least 3.

5 SIMULATION

In this simulation, the sensor network is composed of $M = 8$ homogeneous sensors with 1 ns sensor noise ($\sigma_u = 0.3$ m). Each sensor receives the signal from the target periodically with a frequency of $f_0 = 30\,Hz$. The sensors are divided into two groups (the first layer and the second layer) and mounted on different altitudes for target height estimation. In order to improve target observability condition, the sensors at two layers are mounted at different positions in x and y axes as shown in Fig. 4. The length, width and height of the surveillance region are 25 m, 12 m and 15 m, respectively.

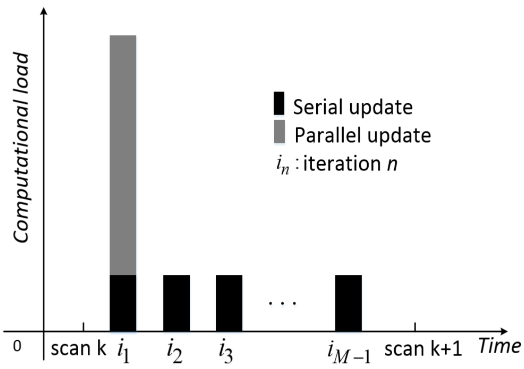

Figure 3: An example of computation distributions of parallel update and serial update.

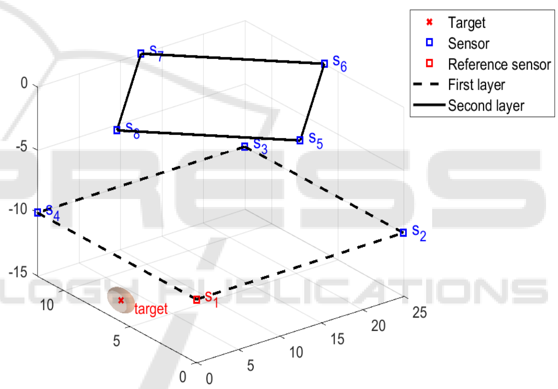

Figure 4: An example of target to sensors geometry in the UWB target tracking system.

For target tracking using TDOA measurements, the Cramer-Rao lower bound (CRLB) (Yang and Scheuing, 2006)(Lui and So, 2009)(Isaacs et al., 2009) indicates the best theoretical performance of filters for the root mean squared error (RMSE) metric. The CRLB value at scan k can be calculated by

$$CRLB_k = \sqrt{J_k^{-1}(1,1) + J_k^{-1}(2,2) + J_k^{-1}(3,3)}, \quad (28)$$

and $J_k^{-1}(i,j)$ indicates the (i,j)th element in the inverse of the Fisher information matrix J_k where

$$J_k = H_k^T R_k^{-1} H_k. \quad (29)$$

In order to evaluate if the sensors are placed properly, a CRLB distribution is mapped by a collection of the CRLB values over all positions. In the CRLB distribution of the scenario, the $x-y$ plane is turned into a grid with a scale of 0.2 m. The height of the emitter equipped on the target is set to be at 1.4 m. Sensor s_1 is predefined as the reference sensor. The result in Fig. 5, in which most of the surveillance area is shadowed in blue, suggests that the theoretical estimation error is small and the sensors are deployed appropriately.

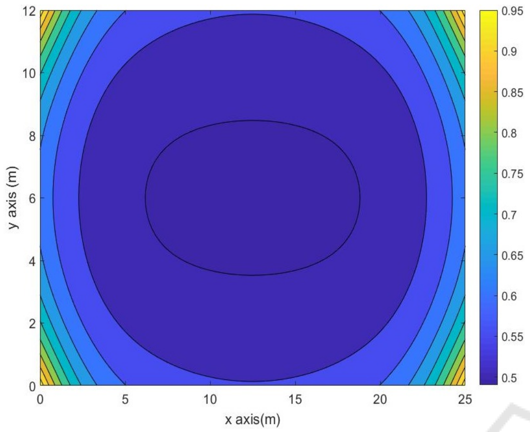

Figure 5: CRLB of the TDOA scenario.

To validate the effectiveness of the proposed approach, the EKF for target tracking using decorrelated TDOA measurements (D-EKF) with different update schemes are simulated. The simulation results obtained from the parallel update and the serial update are denoted as EKF parallel and D-EKF serial, respectively. The simulation tests $N = 100$ Monte Carlo runs and the total simulated time in one run is 40 s. The sampling time is $T_s = 1/f_0$. Sensor s_1 performs as the reference sensor and all the other sensor measurements are assumed to be available in the entire simulated time. The target starts from an initial position $[0\ 6\ \text{-}13.6]^T$ m and moves with speed $[0.5\ 0\ 0]^T$ m/s and follows the dynamics of (1) with

$$F_k = \begin{bmatrix} I_3 & T_s I_3 \\ 0_3 & I_3 \end{bmatrix}, \ Q_k = \sigma_\omega^2 \begin{bmatrix} \frac{T_s^4}{4} I_3 & \frac{T_s^3}{2} I_3 \\ \frac{T_s^3}{2} I_3 & T_s^2 I_3 \end{bmatrix}, \quad (30)$$

where the standard deviation of the process noise is $\sigma_\omega = 0.707\ m/s^2$. The tracking performance is evaluated by RMSE, which indicates the accuracy of the estimated target trajectory. The RMSE in position at scan k is given by

$$\text{RMSE}_k = \sqrt{\frac{1}{N}\sum_{n=1}^{N}\left((x_k-\hat{x}_k)_n^2+(y_k-\hat{y}_k)_n^2+(z_k-\hat{z}_k)_n^2\right)}. \quad (31)$$

As can be seen in Fig. 6, the RMSE curves for EKF parallel and D-EKF serial indicate that the tracking performances are similar. The RMSE curves also demonstrates that the parallel update and the serial update cannot achieve identical results in nonlinear systems. In the parallel update, H_k^p is the linearization of the nonlinear function $h(x_k)$ and is calculated by differentiating w.r.t the predicted state $\bar{x}_k$. In the serial update, the predicted state $\bar{x}_k$ changes at each iteration, which leads to a different linearization error compared with the parallel update. Consequently, the tracking performance of the parallel update becomes different from the serial update. The averaged RMSE of is around 0.15 m that the TDOA measurement noise ($\sqrt{2}\sigma_u \approx 0.42\ m$) is filtered effectively and the target trajectory is estimated accurately.

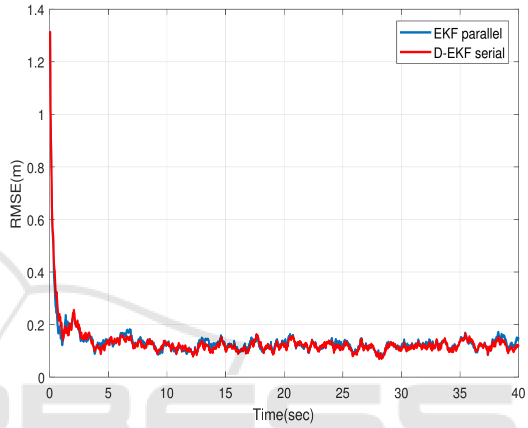

Figure 6: RMSE comparison.

The simulation studies are conducted on a Windows 7 platform (Intel i7-6700 CPU, 16.0 GB RAM) and run with the MATLAB program. The execution time comparison in Table 1 reveals that the parallel update method requires more execution time (even cannot operate in real-time regarding to $T_s \approx 0.0333$ sec) compared to the serial update, which makes it inappropriate for practical installations. By avoiding the complicate matrix operations in high matrix dimensions and utilizing the sensor measurements sequentially, the serial update enables to operate in real-time while distributes the computational load uniformly.

Table 1: Execution time for one sampling interval ($T_s = 1/f_0 \approx 0.0333$ sec).

Method	Parallel	Serial	One iteration
Time (sec)	0.0534	0.0125	0.0017

6 CONCLUSION

This paper presents an effective method which utilizes the serial update and the Cholesky decomposition for target tracking with the multi-sensor TDOA measurements under the correlated measurement noises condition. The serial update scheme, which not only consumes less memory storages but also less computational resources, is adopted in this paper. To obtain an equivalent transformation from the parallel update to the serial update, the inherent correlation between TDOA measurement noise should be appropriately considered. In the proposed D-EKF, the Cholesky decomposition is applied to convert the correlated noise into an pseudo uncorrelated one for the EKF serial update. The simulation result shows that similar tracking performances are obtained under different execution time, which demonstrates the computational efficiency of the proposed method.

ACKNOWLEDGEMENT

This work was conducted at High-speed Vehicle Research Center of KAIST with the support of Defense Acquisition Program Administration (DAPA) and Agency for Defense Development (ADD).

REFERENCES

Alarifi, A., Al-Salman, A., Alsaleh, M., Alnafessah, A., Al-Hadhrami, S., Al-Ammar, M. A., and Al-Khalifa, H. S. (2016). Ultra wideband indoor positioning technologies: Analysis and recent advances. *Sensors*, 16(5):707.

Bar-Shalom, Y., Li, X. R., and Kirubarajan, T. (2004). *Estimation with applications to tracking and navigation: theory algorithms and software*. John Wiley & Sons.

Bar-Shalom, Y., Willett, P. K., and Tian, X. (2011). *Tracking and data fusion*. YBS publishing.

Challa, S., Mušicki, D., Morelande, M. R., and Evans, R. J. (2011). Fundamentals of object tracking.

Duan, Z., Han, C., and Tao, T. (2004). Optimal multi-sensor fusion target tracking with correlated measurement noises. In *Systems, Man and Cybernetics, 2004 IEEE International Conference on*, volume 2, pages 1272–1278. IEEE.

Duan, Z., Li, X. R., Han, C., and Zhu, H. (2005). Sequential unscented Kalman filter for radar target tracking with range rate measurements. In *Information Fusion, 2005 8th International Conference on*, volume 1, pages 8–pp. IEEE.

Eryildirim, A. and Guldogan, M. B. (2016). A Gaussian mixture Bernoulli filter for extended target tracking with application to an ultra-wideband localization system. *Digital Signal Processing*, 57:1–12.

Gan, Q. and Harris, C. J. (2001). Comparison of two measurement fusion methods for Kalman-filter-based multi-sensor data fusion. *IEEE Transactions on Aerospace and Electronic systems*, 37(1):273–279.

Gillette, M. D. and Silverman, H. F. (2008). A linear closed-form algorithm for source localization from time-differences of arrival. *IEEE Signal Processing Letters*, 15:1–4.

Hashemipour, H. R., Roy, S., and Laub, A. J. (1988). Decentralized structures for parallel Kalman filtering. *IEEE Transactions on Automatic Control*, 33(1):88–94.

Ho, K. and Chan, Y. (1993). Solution and performance analysis of geolocation by TDOA. *IEEE Transactions on Aerospace and Electronic Systems*, 29(4):1311–1322.

Isaacs, J. T., Klein, D. J., and Hespanha, J. P. (2009). Optimal sensor placement for time difference of arrival localization. In *Decision and Control, 2009 held jointly with the 2009 28th Chinese Control Conference. CDC/CCC 2009. Proceedings of the 48th IEEE Conference on*, pages 7878–7884. IEEE.

Kaune, R., Hörst, J., and Koch, W. (2011). Accuracy analysis for TDOA localization in sensor networks. In *Information Fusion (FUSION), 2011 Proceedings of the 14th International Conference on*, pages 1–8. IEEE.

Kim, W. C., Song, T. L., and Mušicki, D. (2012). Mobile emitter geolocation and tracking using correlated time difference of arrival measurements. In *Information Fusion (FUSION), 2012 15th International Conference on*, pages 700–706. IEEE.

Lui, K. W. and So, H.-C. (2009). A study of two-dimensional sensor placement using time-difference-of-arrival measurements. *Digital Signal Processing*, 19(4):650–659.

McCracken, M., Bocca, M., and Patwari, N. (2013). Joint ultra-wideband and signal strength-based through-building tracking for tactical operations. In *Sensor, Mesh and Ad Hoc Communications and Networks (SECON), 2013 10th Annual IEEE Communications Society Conference on*, pages 309–317. IEEE.

Pao, L. Y. and Frei, C. W. (1995). A comparison of parallel and sequential implementations of a multisensor multitarget tracking algorithm. In *American Control Conference, Proceedings of the 1995*, volume 3, pages 1683–1687. IEEE.

Pao, L. Y. and Trailovic, L. (2000). The optimal order of processing sensor information in sequential multisensor fusion algorithms. *IEEE Transactions on Automatic Control*, 45(8):1532–1536.

Taylor, J. D. (1994). *Introduction to ultra-wideband radar systems*. CRC press.

Tuchler, M., Schwarz, V., and Huber, A. (2005). Location accuracy of an UWB localization system in a multipath environment. In *Ultra-Wideband, 2005. ICU 2005. 2005 IEEE International Conference on*, pages 414–419. IEEE.

Xie, Y., Lee, H., Ahn, M., Lee, B. J., and Song, T. L. (2016). Joint integrated track splitting for multi-sensor multi-target tracking in clutter. In *Proceedings of the 13th International Conference on Informatics in Control, Automation and Robotics*, pages 299–307. SCITEPRESS-Science and Technology Publications, Lda.

Yang, B. and Scheuing, J. (2006). A theoretical analysis of 2D sensor arrays for TDOA based localization. In *Acoustics, Speech and Signal Processing, 2006. ICASSP 2006 Proceedings. 2006 IEEE International Conference on*, volume 4, pages 901–904. IEEE.

You, H., Dajin, L., and Yingning, P. (1999). State estimation for multilevel multisensor data fusion systems. *ACTA ELECTRONICA SINICA*, page 08.